*Solar Energy* Vol. 52, No. 1, pp. 9–25, 1994
Printed in the U.S.A.

0038-092X/94 $6.00 + .00


# ANALYSIS METHODOLOGY, EXPERIMENTAL INVESTIGATION, AND COMPUTER OPTIMIZATION OF A PASSIVE SOLAR COMMERCIAL BUILDING IN THE BELGIAN CLIMATE

PH. ANDRE, J. NICOLAS,* J. F. RIVEZ, and V. DEBBAUT
Fondation Universitaire Luxembourgeoise, Arlon-Belgium

**Abstract**—The Fondation Universitaire Luxembourgeoise (FUL) building (completed in 1986) has been selected as a Belgian candidate for participation in the IEA (International Energy Agency) Task XI project devoted to passive solar commercial buildings. Therefore, an evaluation methodology has been set up and a monitoring plan has been defined and performed. Together with this experimental investigation, intensive computer simulation work has defined an optimized design of the building. The main results show that the recorded performance can be improved to an extent of 15% energy savings, which yields a correct performance for a passive solar building in the temperate maritime Belgian climate.

## 1. INTRODUCTION

Since 1983, the Fondation Universitaire Luxembourgeoise (FUL) Research Institute, situated in Arlon, in the southern part of Belgium, has used active solar buildings integrating solar collectors, heat pump systems, and in-ground energy storage devices. The performance of these buildings has been described in an earlier paper[1]. In 1985, the institute decided to plan a new building in order to provide rooms for educational use: amphitheaters, offices, and meeting rooms. As solar energy was one of the main research areas of the institute, a passive solar design was naturally selected in order to reduce the auxiliary heating load of the building. A high thermal inertia was chosen by combining mass walls with a high thermal insulation level. This building (Fig. 1) has been extensively analyzed in the context of an international collaboration project, namely the IEA (International Energy Agency) task XI (Implementing Agreement on Solar Heating and Cooling), devoted to "passive and hybrid solar systems for commercial buildings." This article reports on the main results of this work. After a short building description, the specifically developed analysis methodology is presented. Then the monitoring plan, methods, and results are described. Simulation tools are used in order to optimize the building design. As a conclusion, some recommendations or design guidelines are given for the architects and designers.

## 2. BUILDING DESCRIPTION

### 2.1 *Location*

The building is situated in a peripheral area of Arlon, a small town in South Belgium. It was built on a horizontal surface, close to a highway. There is no material obstruction to solar radiations until the end of the afternoon when the sun disappears behind surrounding buildings (for further description, see IEA's Task XI, *Basic Case Studies*[2]).

### 2.2 *Form*

The building has a rectangular (30 × 14 m) shape. This two-storied building is elongated from east to west and the southern facade has a trapezoidal shape with a maximum height of 10.75 m. The first storey (Fig. 2) consists of two amphitheaters enclosing a central hall. The second storey (Fig. 3) includes two meeting rooms and several offices enclosing the same hall. The amphitheaters, offices and meeting rooms are separated from the glazed south facade by concrete mass walls and narrow sunspace areas. The building cross section (Fig. 4) is trapezoidal with a height continuously decreasing from 10.75 m (south facade) to 4 m (north facade).

### 2.3 Construction

The structure of the building is composed of load-bearing masonry walls with an insulating material (thickness = 12 cm) and a covering material for rain protection. The south-faced side is highly glazed: the glazed fraction is 66% of the total southern facade. Concrete mass walls are situated behind the glazing and have both a thermal storage and a load-bearing function. The north-faced side is insulated and consists of load-bearing concrete walls. The windows are made of double high emissivity glazing with aluminium frame. The insulating material of walls, roofs, and floors is glass wool. The typical U-values in $W/m^2$ K are 0.41 (floor), 0.28 (walls), 3.02 (windows), and 0.18 (roofs). This yields an envelope heat loss factor of 1.6 kW/K for transmission through the fabric.

### 2.4 *Services*

The direct gain rooms are partly heated by solar radiation. The concrete walls provide short-term heat storage for amphitheaters, meeting rooms, and offices and dampens the temperature fluctuations. Addition-

* ISES member.

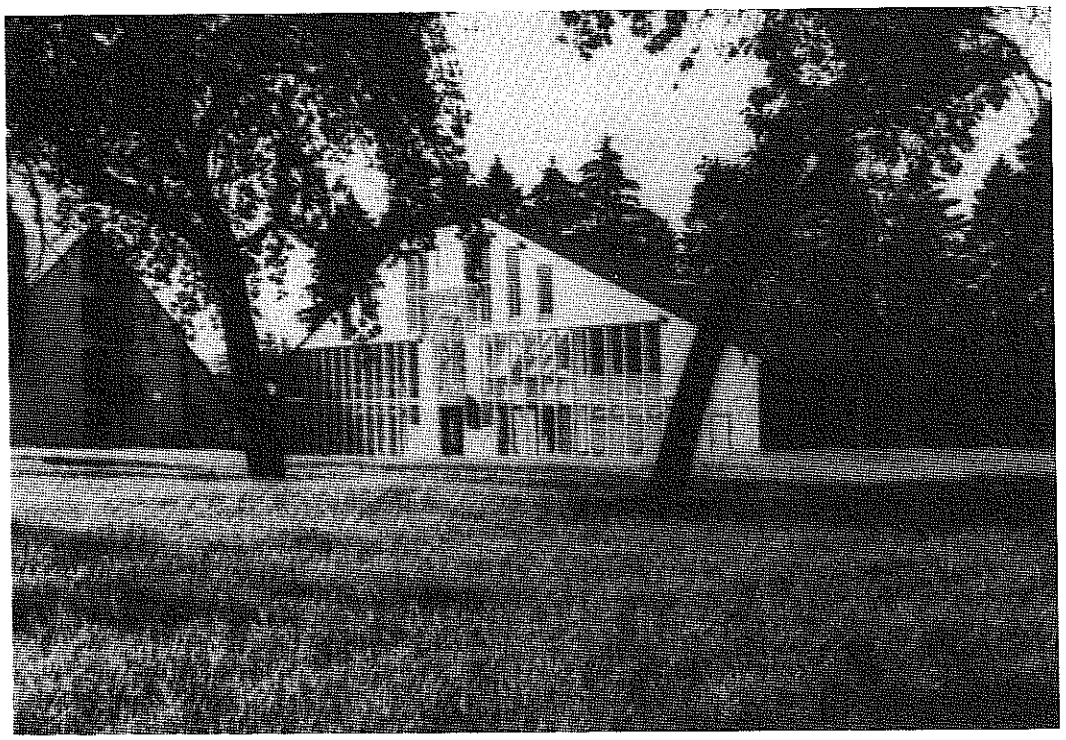

Fig. 1. View of the FUL building.

ally, heating is produced by an auxiliary gas-fired boiler and distributed by thermostatically controlled radiators. In case of overheating or air pollution, ventilation is automatically activated in amphitheaters and meeting rooms. The glazed facade is provided with external roller-blinds, which are activated during the night, in order to reduce the heat losses, and during overheating periods. No centralized computer control of the building is provided even though the heating, ventilating, and shading systems are partly automatically controlled.

2.5 *Solar features*

The main passive solar feature consists of two mass walls situated in the southern facade and separated by a direct gain central zone. Each mass wall is composed by a glazing with an external shading device, a buffer space, and a thermal accumulation wall. The total glazing area is 135 $m^2$, representing 66% of the south facade. The solar radiation is collected through the glazing and accumulated in the wall. Long-wave radiations are exchanged between the wall and the glazing and increase wall surface and, by convection, air tem-

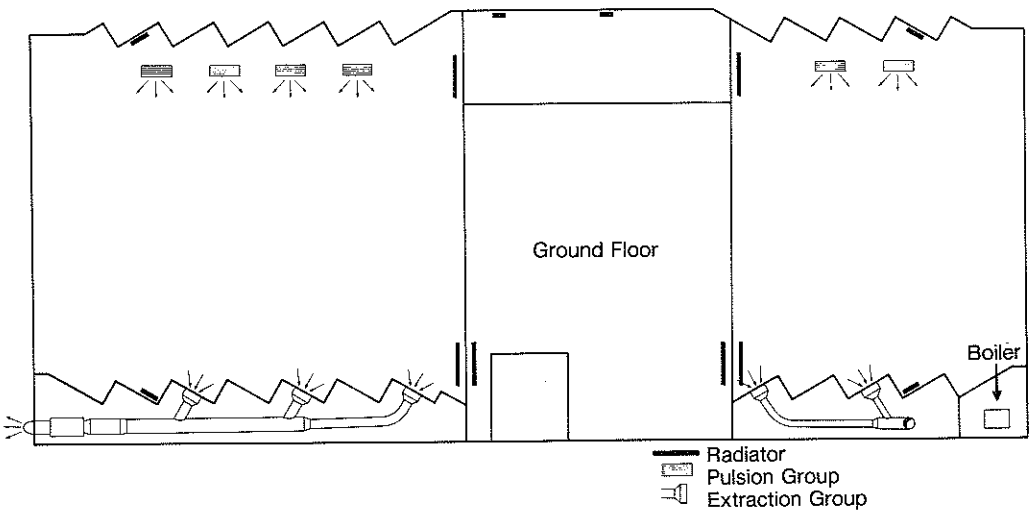


Fig. 2. Floor plan of the FUL building ground floor.

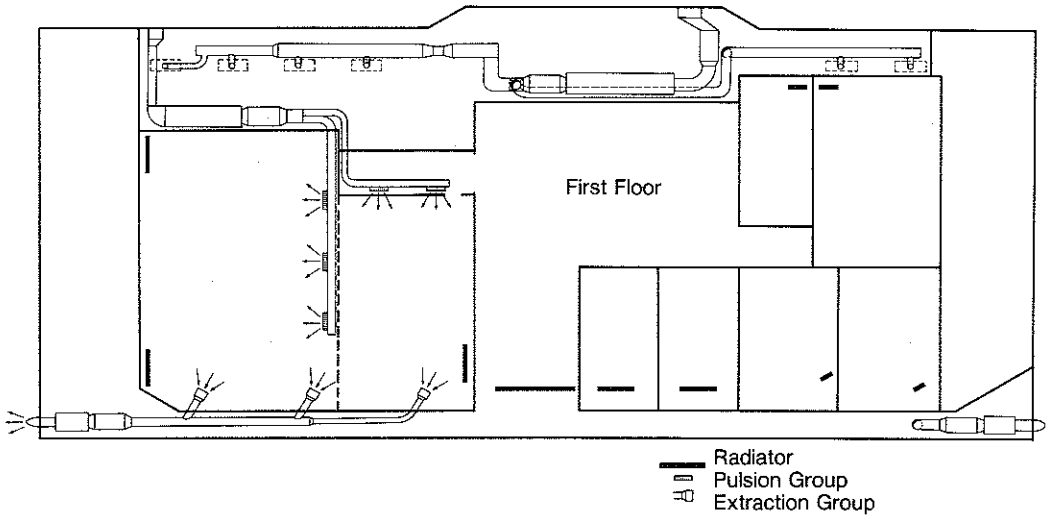


Fig. 3. Floor plan of the FUL building 1st floor.

peratures. The heat is slowly conducted through the wall and released, with a timeshift, to the rooms to be heated. The overall heat transfer process is depicted by Fig. 5. The glazing is double without low-emissivity coating. The walls are painted white even though this color is not optimal for the purpose of solar collection. The walls are composed by a combination of L-shaped concrete elements, separated between each other by interior windows. Additional interior windows are integrated in the concrete elements themselves at the secondary storey in order to provide some more daylighting in the offices and meeting rooms. The external shading device is automatically activated during the night, during the weekend in winter, and can be partly lowered manually by the occupants in case of overheating.

Thermal mass is present in the direct gain central zone as well: the floor and the ceiling are made of reinforced concrete and an additional concrete beam has been placed horizontally at the first storey, behind the glazing. The combination of thermal mass and high insulation level leads to a high thermal inertia characteristic for this building.

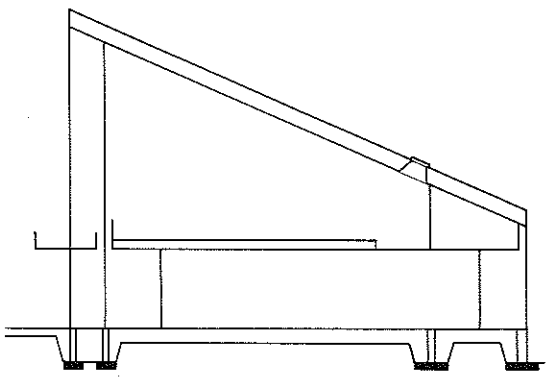

Fig. 4. Cross section of the FUL building.

## 3. ANALYSIS METHODOLOGY

A specific methodology has been proposed to analyze the building. It combines both an experimental procedure and computer simulations in order to learn as much as possible from this project and to make this knowledge useful and usable for future projects.

The methodology can be seen as a three-point strategy which is directly connected to the organization of the IEA task XI project. The first step of the strategy concerns the experimental investigation of the building. Therefore, a monitoring plan has been defined, instrumentation of the building has been set up, and measurements have been performed according to this monitoring plan. The measurements were handled by several analysis software programs: statistical, graphical, and process-identification oriented.

The second step of the strategy is more concerned with a theoretical investigation of the system based upon a computer description of the building. This approach includes several orientations. First, a validation of the different simulation tools used to model this building had to be performed. Therefore, the building was simulated with real (measured on site) climatic and occupation data. Based upon different two-week-long periods, the comparison between measured and calculated indoor temperatures yields an impression of how the model is able to simulate the building. The second step concerns the calibration of the model. This involves the selection of accurate values for some typical parameters, among others the heat exchange coefficients of the model. Therefore, simplified mathematical models of some local thermal processes are defined (surface heat balances, thermal conduction, etc. . . .) and system identification algorithms are used to perform the parameters calculation. The combination of both approaches establishes a two-way communication between model and measurements: the monitoring improves the model (calibration) and the

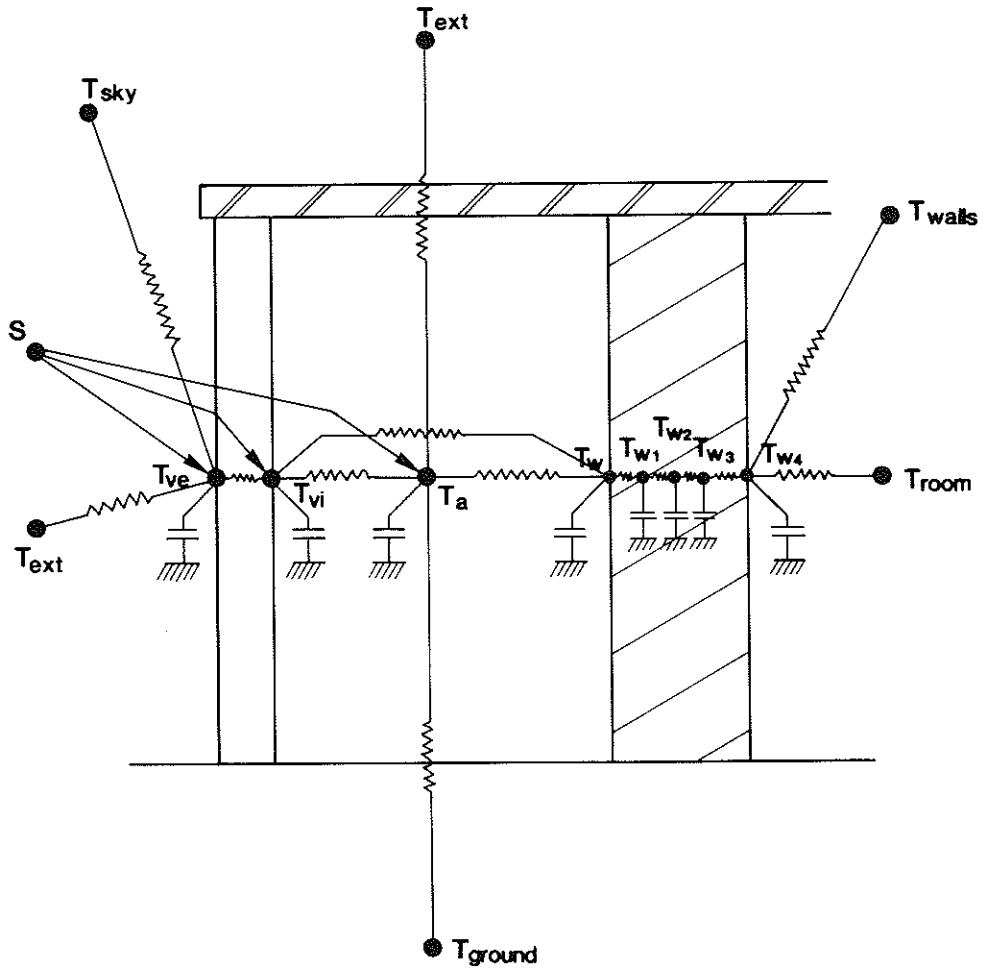


Fig. 5. Heat transfer in the mass wall system.

model helps define a better monitoring strategy. This makes the strategy a dynamic evolutive one.

These two strategies are directed toward the third step which can be seen as the output part, namely the definition of design guidelines based upon the "lessons" of the monitoring and the insights of the simulation results. This makes the overall knowledge obtained during the project useful for the design of future buildings.

The overall strategy is schematically represented in Fig. 6. As shown by this figure, the output provides results expressed as design guidelines or recommendations for architects or building designers: what to do or/and what not to do in several situations. An alternative method for the presentation of the results consists of an expert system in which rules are implemented to summarize the different design guidelines. This implementation work has been performed in the context of the Task XI project, and the expert system software "ISOLDE"[3]is associated with a videotape presentation of built projects aiming at illustrating the different passive solar strategies.

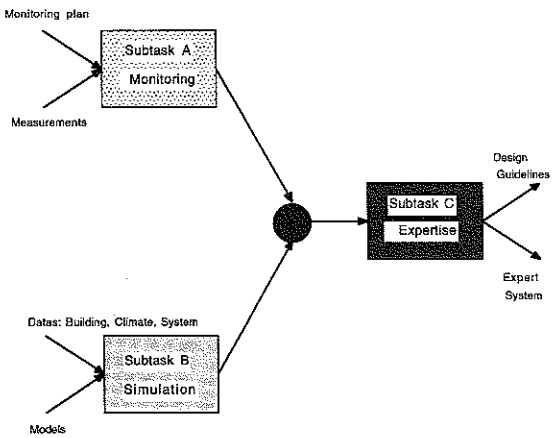


Fig. 6. Overall strategy for the analysis methodology of the FUL building.

## 4. PRELIMINARY ANALYSIS OF THE BUILDING

A preliminary analysis of the building has been performed in order to define the monitoring plan and strategies and to determine the overall time schedule of the study. This analysis is based upon the division

of the building in components whose definition is closely related to the interaction between the different passive solar devices, the environmental influences, the auxiliary HVAC system, and, finally, the overall control system. This division yields the following components:

- environmental variables:
  external environment: climate
  internal environment: occupants,
- glazing and associated shading device,
- buffer space,
- storage wall,
- passively heated rooms (the whole building without the mass walls),
- building envelope,
- auxiliary heating system,
- mechanical ventilation system, and
- control systems.

For each component, the evaluation plan has defined four items to be considered:

1. aims of the analysis,
2. methods to be used:
   measurements
   simulations
   combination of both,
3. tools:
   sensors
   simulation and analysis softwares
   inquiries about occupants behaviour and opinion, and
4. evaluation: what are the expected results of the analysis, how is it possible to give an interpretation of the results?

The design of the monitoring has been selected in order to meet the requirements of the proposed analysis. The instrumentation of the building has been realized in conformity with the subsystems division. The glazing, buffer sunspace, and accumulation wall received special attention as they are the main passive solar features of the building. The monitoring period was first scheduled for one year, but several problems with the auxiliary heating system made a second year necessary in order to get reliable information from the measurements. Furthermore, some "one-time" measurements were planned: infrared thermographic analysis, pressurization test, heat fluxes measurements. These tests aimed at a better knowledge of how the building was responding to the action of environmental variables.

## 5. MEASUREMENTS

The measurements [4] were planned with the following objectives:

1. Evaluation of the thermal performance of the building. Determination of the passive solar heating contribution of the mass wall to the heating load.
2. Validation of the Belgian computer model "MBDSA" against the data recorded *in situ*. This was useful in order to determine whether the software "MBDSA" was suitable for the simulation of passive solar commercial buildings including indirect gain and direct gain features.
3. Determination of heat exchange coefficients in the mass wall system through application of process identification methods. The exchange coefficients of the heat transfer occuring in a mass wall were to be investigated as the values of these coefficients could be substantially different from those of a more classical design.
4. Evaluation, by means of a Fanger-like methodology, of the thermal comfort in the building.

In order to meet these different objectives and following the division of the building into several subsystems, the *a priori* selection of measurement points considered:

- the division of the building in 10 zones in order to allow the comparison of measurements with simulated results (a 10-zone modeling was selected as well);
- the organization of the instrumentation according to the subsystems listed above.

Most of the air temperatures were measured by thermistors (Fenwall UUA41J1). Kipp and Zonen pyranometers were used for the measurement of global and diffuse horizontal radiation. Special hot-wire anemometers were installed in the sunspaces for the measurement of air velocities. The thermistors were factory calibrated and have a 0.2°C error band while the pyramometers error is about 2% for values higher than 100 $W/m^2$. The hot wire anemometers were calibrated in an air-tunnel. The gas (auxiliary energy) consumption was measured by recording the counter number twice a day. The same strategy was used for the global electricity consumption of the building.

### 5.1 *Collection of measurement data*

Approximately 60 sensors were measured during the monitoring period. During the first year of monitoring, the temperature measurements were performed and stored every 15 minutes while solar radiation measurements were scanned every 3 minutes (because of the limitations of the data-acquisition system) and recorded after integration every 15 minutes. Comparisons were made with a one-minute time step in order to check the accuracy of the solar radiation measurements. Considering the time response of the building, they did not point out any significant difference. During the second year of monitoring, the storage period was raised up to one hour. Every one or two weeks, the data were transferred to a PC computer system on which the data processing was performed. Depending upon the objectives, this operation was realized by:

- a process identification (mathematical estimation of parameters in dynamical systems) software ("IDSOFT") developed at FUL [5] in order to estimate heat exchange coefficients in a dynamical process,
- a simple statistical software developed at FUL in order to aggregate the information contained in the data, and
- a graphical software in order to visualize typical monitoring periods and aggregated results.

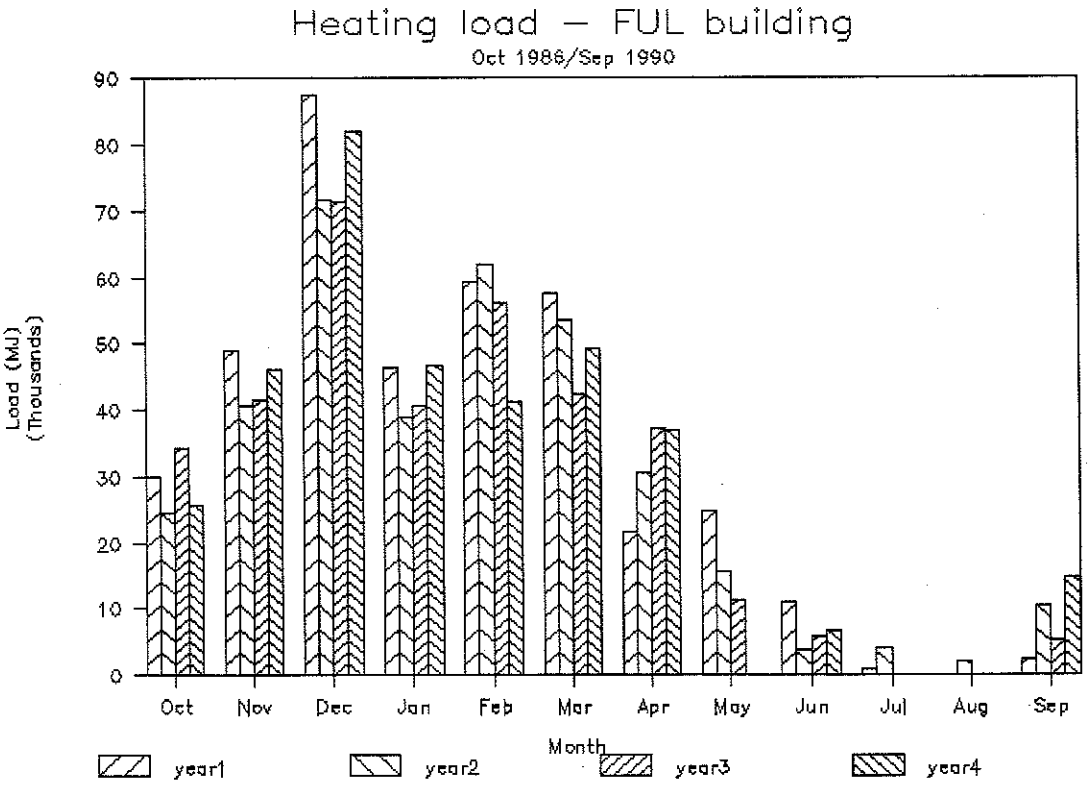


Fig. 7. Monthly distribution of the auxiliary heating load.

5.2 *Energy results*

Table 1 lists the auxiliary heating load for the first four years of occupation of the building (October 1986 to September 1990). The monthly distribution of the auxiliary heating load is given in Fig. 7. January is usually low because, during the last four years this month has been generally mild.

When reduced to gross floor area, these figures yield the values of Table 2. These figures can be seen as quite high for a passive solar building. The first year figure is probably the result of the building drying and the consequence of a winter colder than the other years. The generally high level of the heating load is partly due to a bad control of the auxiliary heating system. Some measurements of the heating system itself have shown that the night and weekend setback strategy of the heating system was not effective, at least for one of the two distribution circuits. This comes from a lack of tightness of a three-way valve which made the heating system work, even during setback periods. The monitoring pointed out the higher temperature of the southern circuit, compared to the northern one during setback periods.

Despite the high insulation level of the building and the passive solar design, the heating load doesn't depict a good overall performance. Another explanation comes from the high value of infiltration losses. A pressurization test performed by the Belgian Building Research Institute has shown the air renewal (by infiltration) in different zones of the building to be:

- auditoriums: 0.3 vol/h
- meeting rooms: 1.25 vol/h
- whole building: 0.65 vol/h.

These figures don't take the mechanical ventilation into account. All zones situated at the upper floor and consequently connected to the roof have a high infiltration rate due to the lack of an air tight layer in the roof.

Figures 8 and 9 show the correlation between the auxiliary heating load and respectively, the ambient temperature and the global horizontal solar radiation,

Table 1. Heating load for four years

| | Heating load | |
|---|---|---|
| Heating season | GJ | kW h |
| 1986/1987 | 391 | 108587 |
| 1987/1988 | 357 | 99181 |
| 1988/1989 | 346 | 96198 |
| 1989/1990 | 349 | 97036 |

Table 2. Heating load per gross floor area for four years

| | Heating load/grass floor area | |
|---|---|---|
| Heating season | $MJ/m^2$ | $kW\ h/m^2$ |
| 1986/1987 | 587 | 163 |
| 1987/1988 | 536 | 149 |
| 1988/1989 | 520 | 144 |
| 1989/1990 | 526 | 146 |

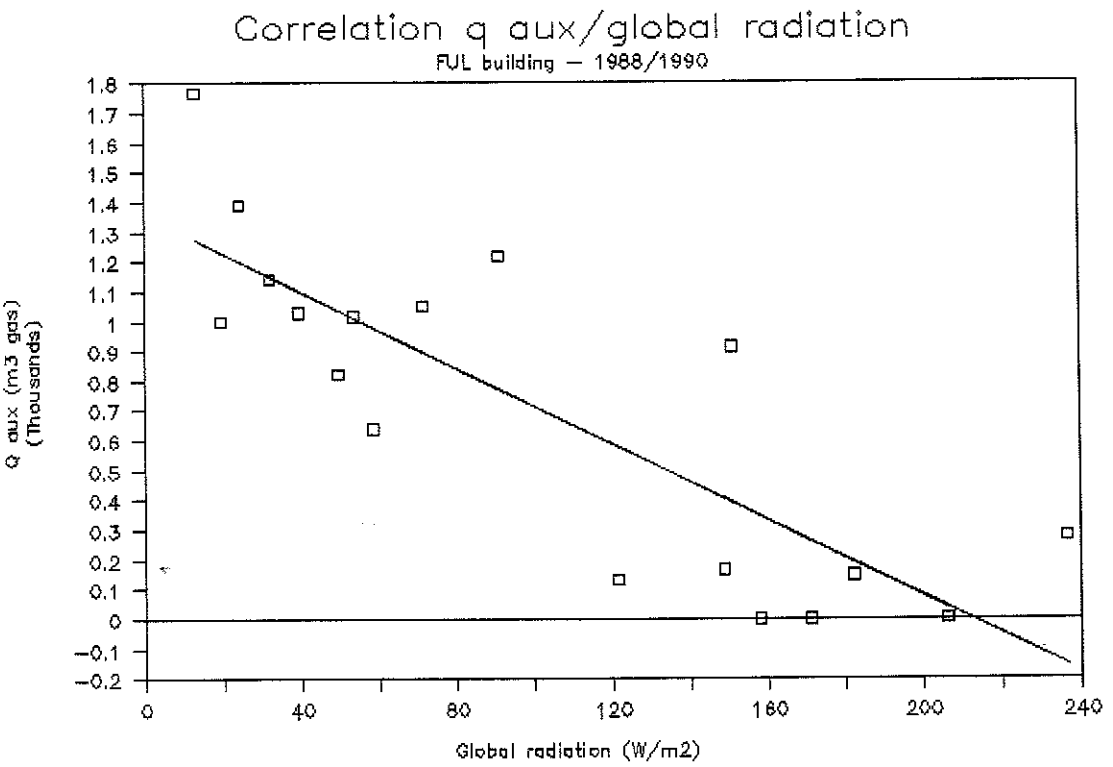


Fig. 8. Correlation between auxiliary heating load and global horizontal solar radiation.

calculated on the basis of monthly average values. Both correlations are not very strong ($R^2$: 0.70 for the ambient temperature; $R^2$: 0.68 for solar radiation) and this relative weakness suggests that other factors (infiltration losses, HVAC control) are influencing the energy consumption of the building.

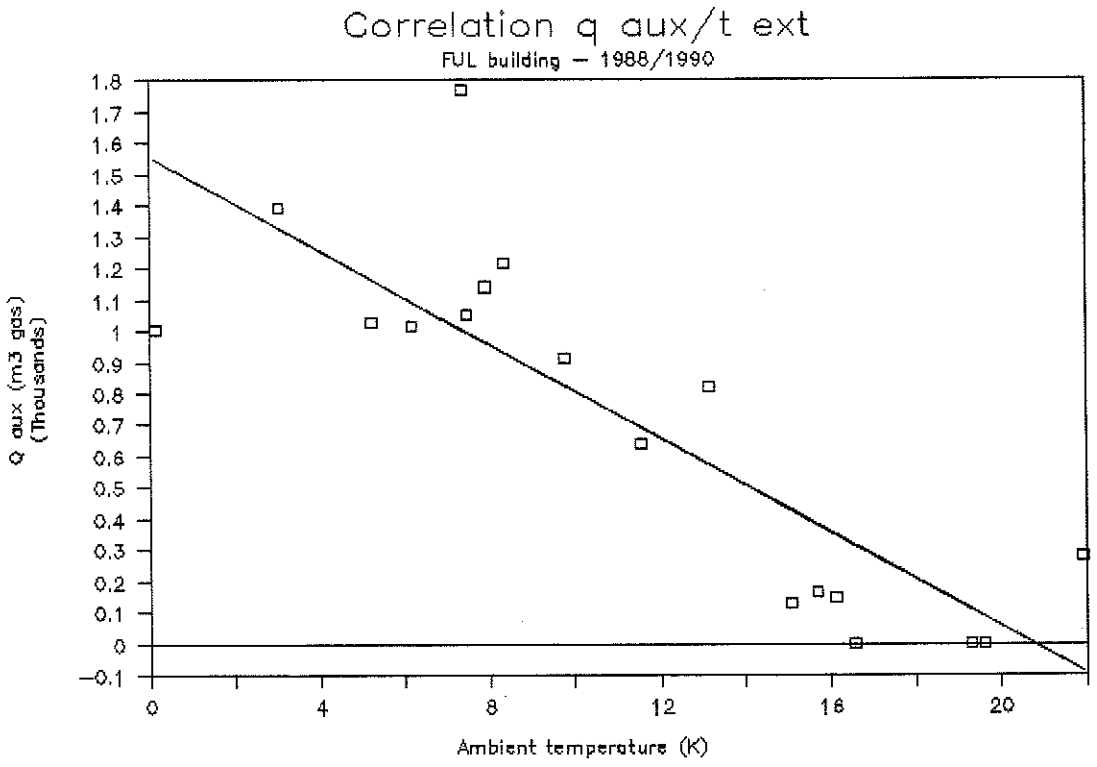


Fig. 9. Correlation between auxiliary heating load and ambient temperature.

Table 3. Average temperature and standard deviations for some zones

| Zone | Average temperature (K) | Standard deviation (K) |
|---|---|---|
| Auditoriums | 19.5 | 0.8 |
| Central hall | 21.5 | 2.3 |
| Offices | 21.7 | 1.5 |
| Visitors offices | 22.7 | 2.0 |
| Meeting rooms | 20.7 | 1.4 |

Table 4. Minimum/maximum temperatures for different zones

| Zone | Minimum temperature (K) | Maximum temperature (K) |
|---|---|---|
| Auditoriums | 13.5 | 27.5 |
| Central hall | 14.6 | 35.7 |
| Offices | 14.3 | 31.3 |
| Visitors offices | 16.9 | 35.8 |
| Meeting rooms | 13.5 | 30.1 |

5.3 *Comfort (amenity)*

The air temperature was recorded in every zone of the building. Averaging the recorded values for two years of monitoring yielded the following figures (Table 3).

This table shows that the average temperatures in the building are quite high, considering the setpoint of the auxiliary heating system to be 21°C during the day. The auditoriums are the coldest zone of the building (because of the reduction of the direct gains) with the lowest deviation around the mean, indicating the damping effect of the mass wall. All solar insolated zones exhibit an average temperature above 20°C with large deviations around the mean, due to both direct solar gains and heating setback. The peak (minimum and maximum) values of the temperatures in the same zone are indicated in the following Table (table 4).

The minimum values are usually associated with the night and weekend setback (although not entirely effective) of the auxiliary heating system while maximum values are the result of a high solar radiation level. These values are usually high, especially if we consider that the rooms are occupied. This shows that overheating is a major problem in this building.

The overheating trend can be further investigated by the computation of temperature frequency distribution diagrams. Figure 10 shows these diagrams for several rooms. Indirect gain zones (auditoriums) exhibit distributions centered around the heating set point and included more underheating than overheating. Direct gain zones show diagrams displaced to the right with a large amount of overheating hours. The calculation of the overall overheating frequency for several typical zones of the building yields the results of Table 5.

This table shows that overheating occurs during a large proportion of occupation hours in the directly insolated zones. Even though the building occupants have the possibility to lower roller blinds in case of overheating feeling, they don't use them very often, probably because they want to keep in touch with the surroundings and benefit from the daylighting associated with solar radiation. Openable windows are located in the roof of the offices area and occupants may

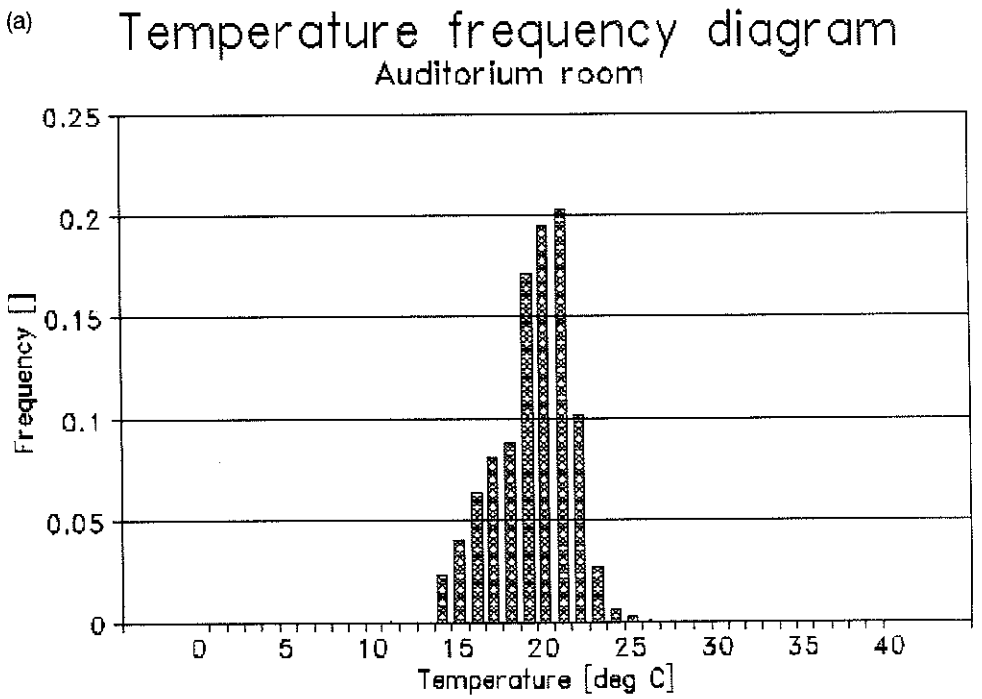


Fig. 10. Frequency distribution for typical zones. (a) Auditorium room.

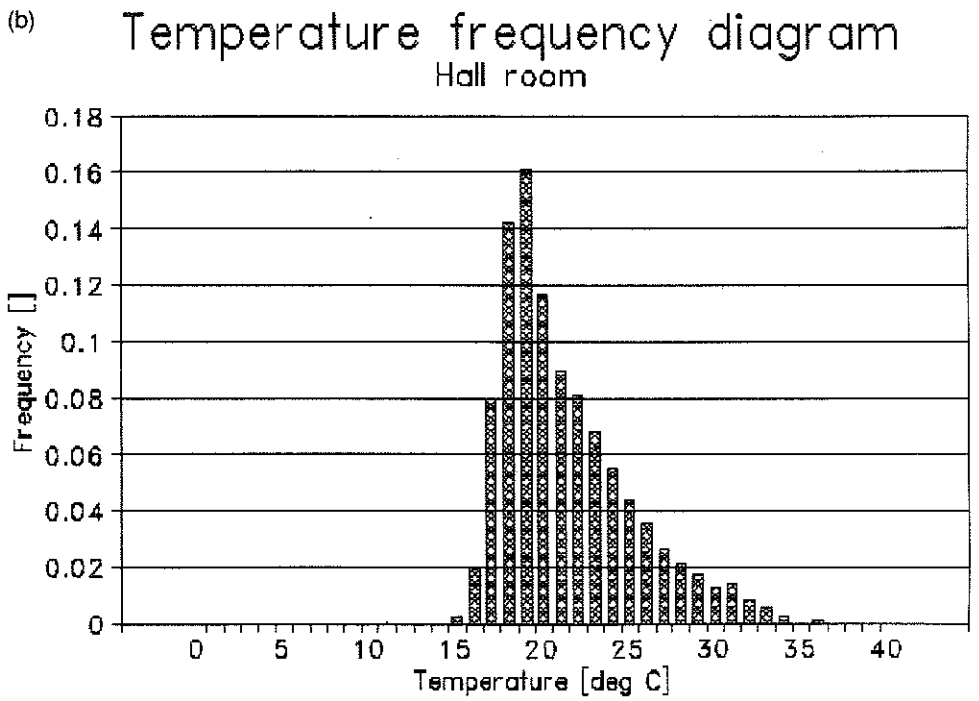


Fig. 10. (*Contd.*). (b) Hall room.

use them in order to increase the infiltration rate of the rooms. But they haven't used them very often, probably because the windows are not very easy to handle. To reduce these overheating problems, an additional mechanical ventilation system has been installed in the offices area. Again, the occupants haven't used this system because of the noise created by the ventilators. This means that the thermal comfort has not to be considered separately but together with other comfort criteria: noise, light, and conviviality.

### 6. SPECIAL FOCUS ON THE MASS WALL

The mass wall has been specially investigated and the detailed results of the research have been included

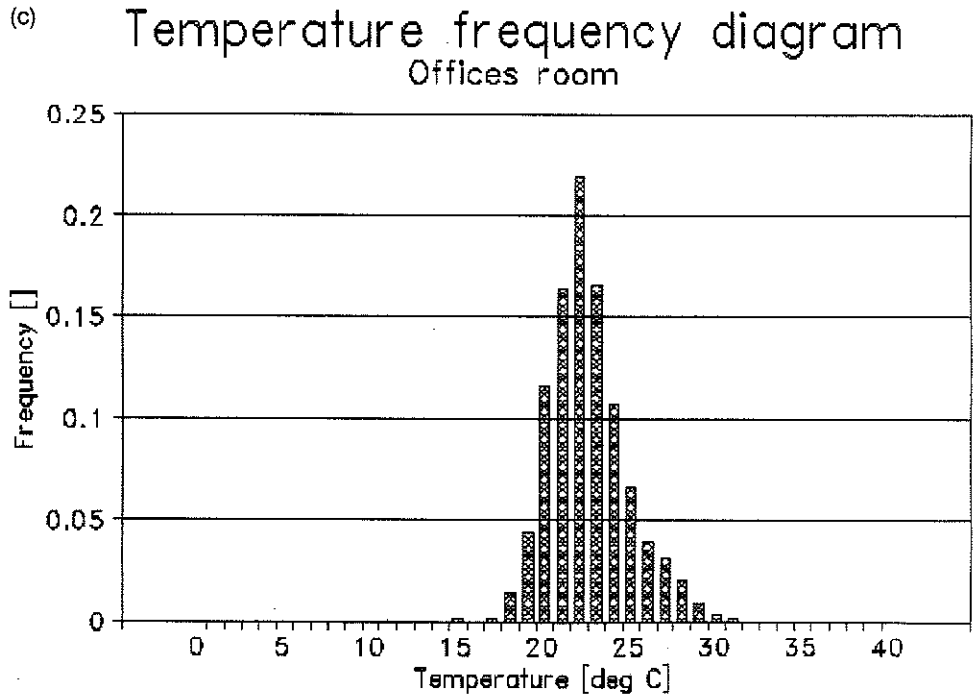


Fig. 10. (*Contd.*). (c) Offices room.

Table 5. Overheating frequency for different zones

| Zone | Overheating frequency (%) |
|---|---|
| Auditoriums | 0.8 |
| Central hall | 24.1 |
| Offices | 27.5 |
| Visitors offices | 35.1 |
| Meeting rooms | 14.8 |

in the IEA Task XI Source Book[6]. Therefore, special attention has been paid to this component in order to measure, analyze, and understand the physical processes occuring in the system.

A theoretical investigation of the mass wall considered as a heating device has been performed. The physical processes occuring in the device have been identified and a simple but reasonably accurate model of the component has been built. This model is described by the thermal network of Fig. 11 and by the following equations set. In this formulation, each equation corresponds to one node of the network. The assumptions of the model are:

- no capacity for glazing and wall surface,
- separated convection and radiation processes,
- linearized long wave radiation, and
- one-dimensional conduction in the wall.

Node 1: energy balance of the external surface of the glazing (no capacity)

$$0 = A_{ve}[\alpha_{ve}\cdot F_g(t)S_H + h_{ve}\cdot(T_{ext} - T_{ve}) - \lambda_v/e_v(T_{ve} - T_{vi}) - \varepsilon_{sky}\cdot\varepsilon_{ve}\cdot F'_{sky,ve}\cdot\sigma\cdot(T_{ve} - T_{sky})]. \quad (1)$$

Node 2: energy balance of the internal surface of the glazing (no capacity)

$$0 = A_{vi}[\alpha_{vi}\cdot\rho_{w_0}\cdot\tau_{ve}\cdot F_g(t)\cdot S_H - \lambda_v/e_v\cdot(T_{vi} - T_{ve}) - h_{vi}\cdot(T_{vi} - T_a) - \varepsilon_{vi}\cdot\varepsilon_{w_0}\cdot\sigma\cdot F'_{vi,w0}\cdot(T_{vi} - T_{w_0})]. \quad (2)$$

Node 3: energy balance of the buffer space air

$$V_a(\rho C_p)_a dT_a/dt = A_{vi}\cdot h_{vi}\cdot(T_{vi} - T_a) - A_{w_0}\cdot h_{w_0}(T_a - T_{w_0}) - (UA)_{ground} \times (T_a - T_{ground}) - (UA)_{roof}\cdot(T_a - T_{ext}). \quad (3)$$

Node 4: energy balance of the internal surface (sunspace side) of the mass wall

$$0 = A_{w_0}[\alpha_{w_0}\cdot\tau_{ve}\cdot F_g(t)\cdot S_H + h_{w_0}\cdot(T_a - T_{w_0}) - \lambda_{w_0}/e_{w_0}\cdot(T_{w_0} - T_{w_i}) - \varepsilon_{w_0}\cdot\varepsilon_{vi}\cdot F'_{w_0,vi}\cdot\sigma\cdot(T_{w_0} - T_{vi})]. \quad (4)$$

Node 4 + $i$: conduction through the mass wall

$$V_{w_i}\cdot(\rho C_p)w_i\cdot dT_{w_i}\cdot/dt = A_{w_{i-1}}\cdot[\lambda_{w_{i-1}}/e_{w_{i-1}}\cdot(T_{w_i} - T_{w_{i-1}})] - A_{w_i}\cdot[\lambda_{w_i}/e_{w_i}\cdot(T_{w_{i+1}} - T_{w_i}\cdot)]. \quad (5)$$

Node 4 + $n$ + 1: energy balance of the external (room side) surface of the mass wall

$$0 = A_{w_{n+1}}\cdot[\lambda_{w_{n+1}}/e_{w_{n+1}}\cdot(T_{w_{n+1}} - T_{w_n}) - h_{w_{n+1}}\cdot(T_{w_{n+1}} - T_{room})e_{w_{n+1}}\cdot\varepsilon_{walls} \times \sigma\cdot F'_{w_{n+1},walls}\cdot(T_{w_{n+1}} - T_{walls})]. \quad (6)$$

The purpose of this modeling work was to serve as a mathematical support to perform an estimation of the physical parameters (heat exchange coefficients) of the device. For instance, the estimation of the heat exchange (convection) coefficient at the surface of the mass wall in the sunspace has been performed from the eqn (4). The estimation yields values between 5 W/m$^2$ and 9 W/m$^2$ K as shown by Table 6.

The values are generally higher than standard values for convection coefficients in buildings. The increase in the values is probably to be associated with the intensity of solar radiation reaching the wall, which in-

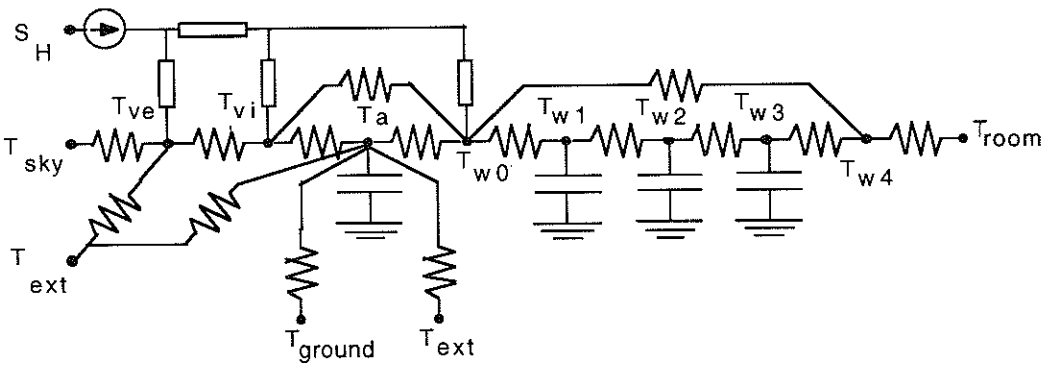


Fig. 11. Thermal network of the mass wall.

Table 6. Convection coefficients in the mass wall system

| Period | Convection coefficient ($W/m^2$ K) |
|---|---|
| (13/06/88–21/06/88) | 6.7 |
| (04/07/88–11/07/88) | 8.9 |
| (12/07/88–18/07/88) | 4.8 |
| (28/07/88–05/08/88) | 7.5 |
| (27/06/89–03/07/89) | 7.8 |
| (03/07/89–13/07/89) | 7.2 |
| (13/07/89–23/07/89) | 6.5 |
| (31/07/89–09/08/89) | 9.1 |

duces thermocirculation effects in the sunspace, thus increasing the heat exchange. The results of the period *nr* 3 confirm this hypothesis: this period was very poorly insolated (cloudy weather) and overcast conditions result in a substantial decrease in the intensity of the heat exchange process[7].

The same procedure has been applied to other parameters, among others to the thermal conductivity of the concrete wall. The overall contribution of the mass wall to the heating of the rooms situated behind it doesn't seem to be very significant. An estimation of the discharge flux of the wall to the auditoriums (Fig. 12) shows that this exchange is negative (i.e., directed from the room to the wall) in winter and during cloudy days. Several reasons may explain the lack of performance of the wall:

- The wall is white. Consequently, most of the solar heat is reflected outside or on the floor.
- The wall is located too far from the glazing: the roof works then as an overhang device when the sun is high.
- The opaque part (34% of the total area) of the facade works as a shading device with respect to the wall when the sun is far from southern azimuth.
- Ventilation ducts are situated in the sunspace. They are painted red and, consequently, absorb more solar energy than the wall itself. Furthermore, they act as a shading device for the wall.
- A general impression, when looking at the wall at several periods of the year, is that the wall is very poorly insolated, because of the several reasons enumerated above. This should have been taken into account in the design.

## 7. SIMULATIONS

The objectives of the simulation work performed in the context of the project were twofold:

1. to validate and/or calibrate a computer model that could be used as a reliable tool for the simulation exercise, and
2. to use a reliable tool in order to perform a systematic parametric analysis of the building in order to establish whether the design is accurate and to derive optimal design guidelines considering both energy and comfort related evaluation criteria.

Two different simulation models of the thermal behavior of multizone buildings have been used in the context of this project: (a) suncode, originally developed at the SERI[8], and (b) MBDSA, a program developed at the University of Liège[9].

As Suncode is unanimously recognized as a suitable tool to simulate passive solar buildings, the challenge

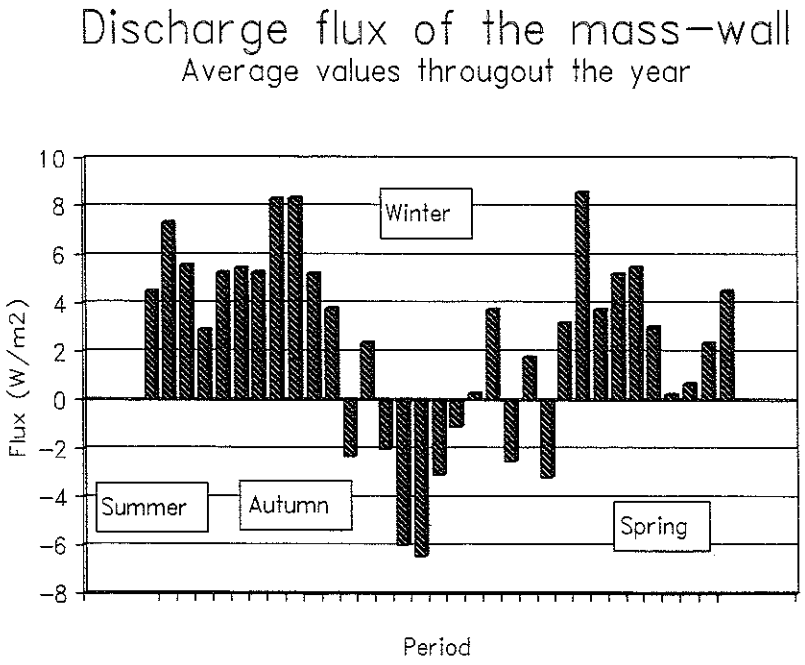


Fig. 12. Discharge flux from the mass wall to the room.

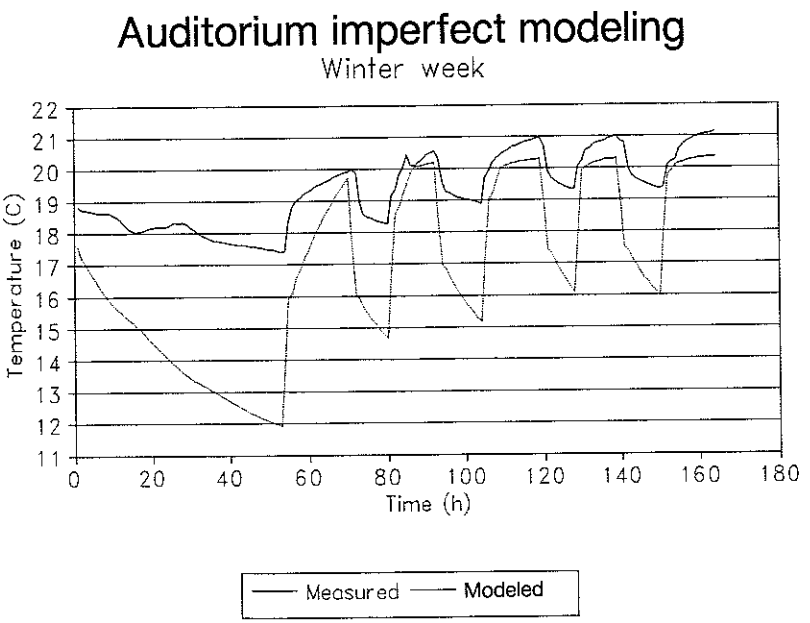


Fig. 13. Auditorium temperature (winter). Nonaccurate heating system modeling.

was to validate MBDSA against both *in situ* measurements and Suncode predictions. Therefore, two typical periods were selected, one in winter (from 04/02/89 to 10/02/89) and one in summer (29/07/88 to 05/08/88). These periods exhibit very different characteristics: the winter period was cold and foggy; the summer one was hot and sunny. The results of this validation exercise were generally good although the winter simulations have shown the big influence of the accuracy of the modeling of the heating system (gas-fired boiler + radiators distribution circuit). Figure 13 shows the auditorium temperature obtained with an approximate modeling of the heating system. Figure 14 shows the same temperature obtained with a more realistic (taking into account losses due to the three-way valve) modeling. The summer simulations showed the generally good accuracy of the MBDSA results compared to the measurements, especially in the sunspaces and mass wall systems (Fig. 15).

Afterward, an additional period was tested, focusing on the mass wall behavior. The wall surface temperatures were checked and, once again, measurements

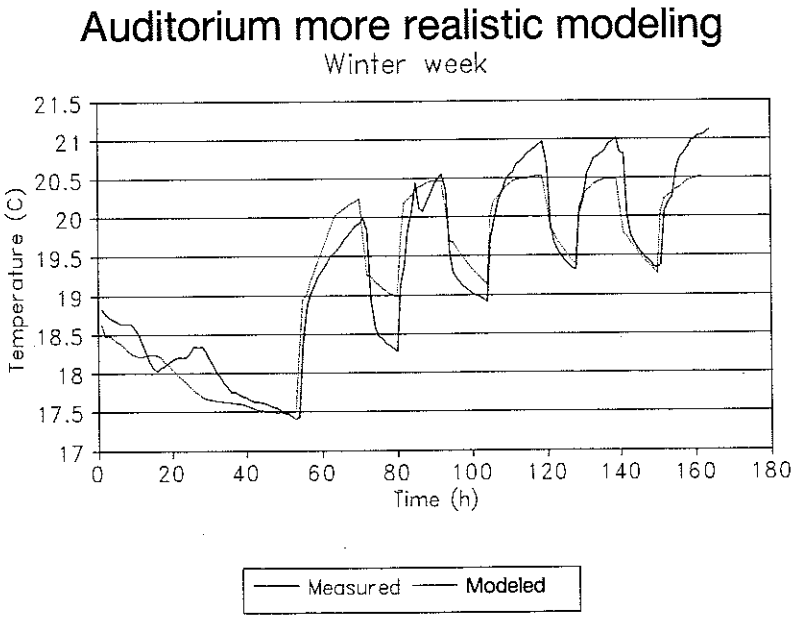


Fig. 14. Auditorium temperature (winter). More realistic heating system modeling.

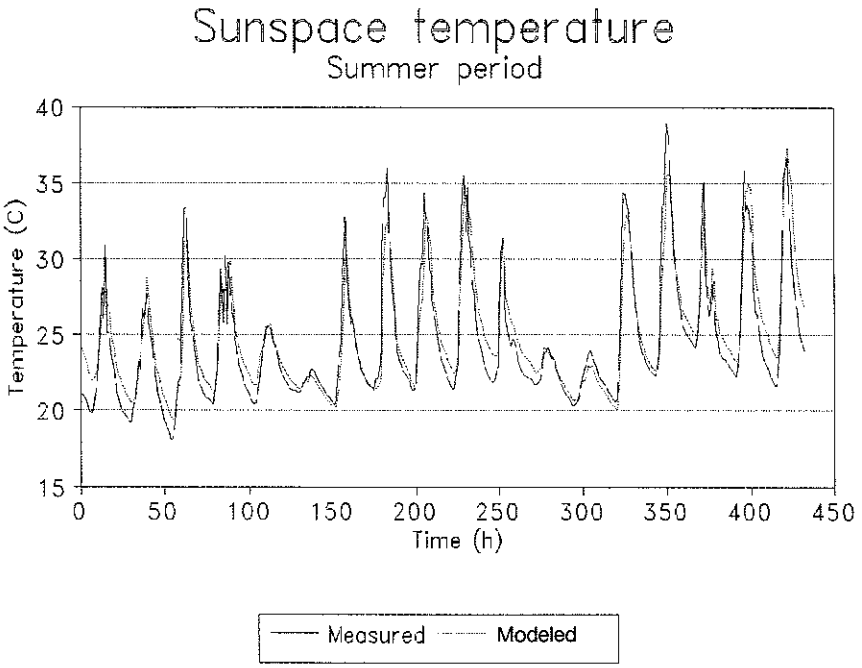


Fig. 15. Sunspace temperature (summer).

and models agreed very well with each other (Fig. 16). This confirms the ability of MBDSA to model passive solar buildings.

The validation step allowed the program to be used for several purposes

- parametric analysis of the building,
- definition of an optimized design, and
- calculation of the solar fraction for several designs.

The parametric analysis of the building concerned the following parameters:

- orientation of the building,
- glazing type,
- buffer space geometry,
- mass wall absorption properties,
- mass wall thickness,
- roller blinds activation strategy,
- south facade glazing area,
- ventilation rate across the wall,
- insulation of the wall,
- storage material, and
- climate.

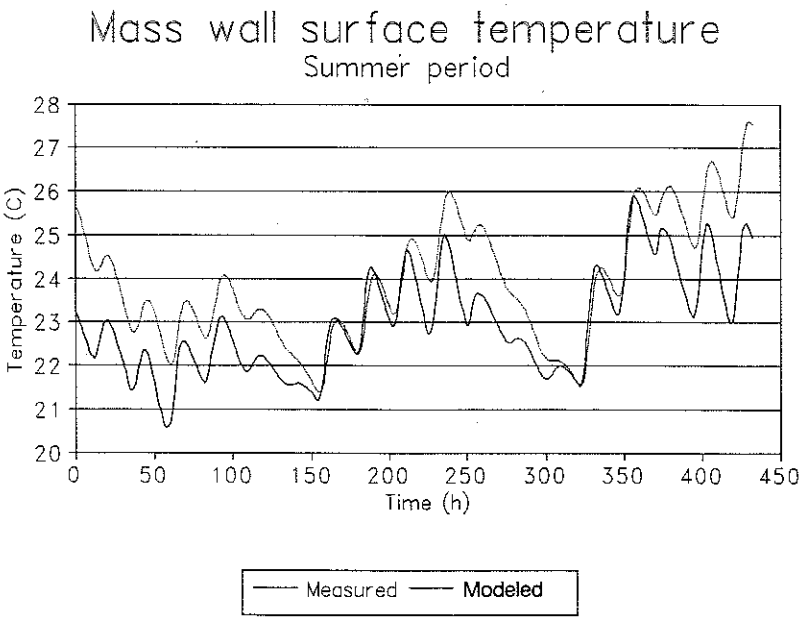


Fig. 16. Mass wall surface temperatures. Model vs. measurements.

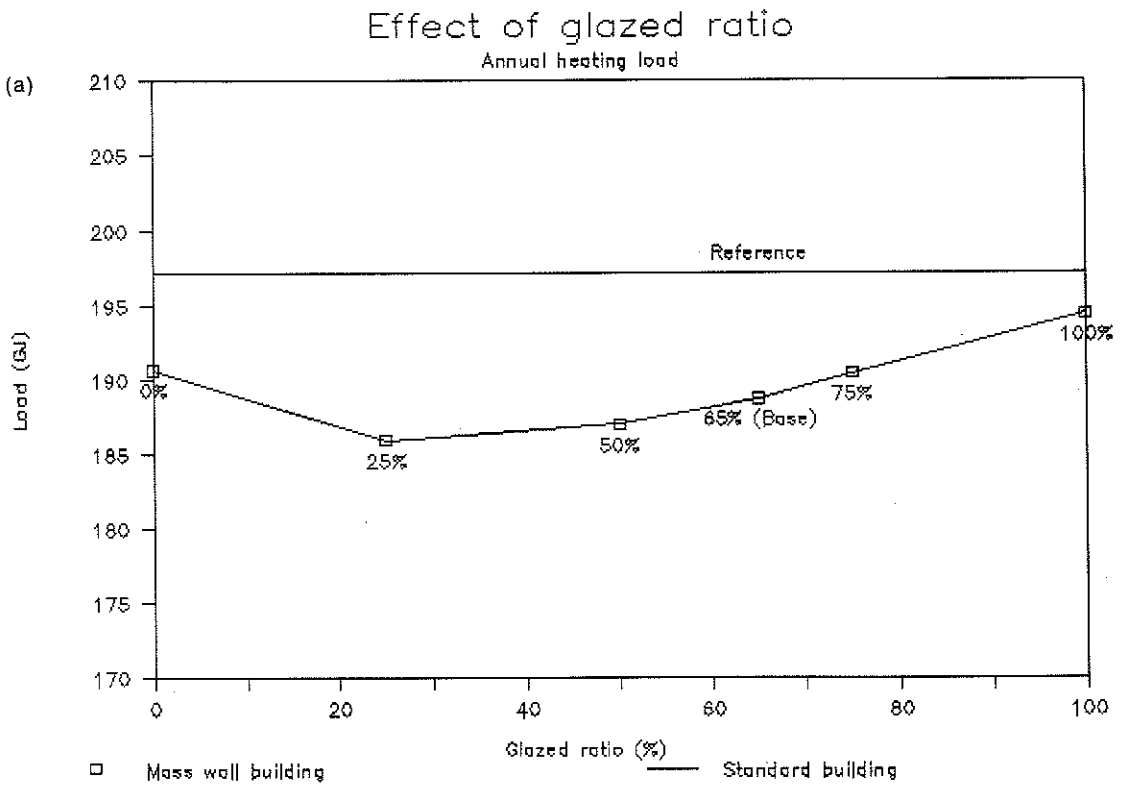


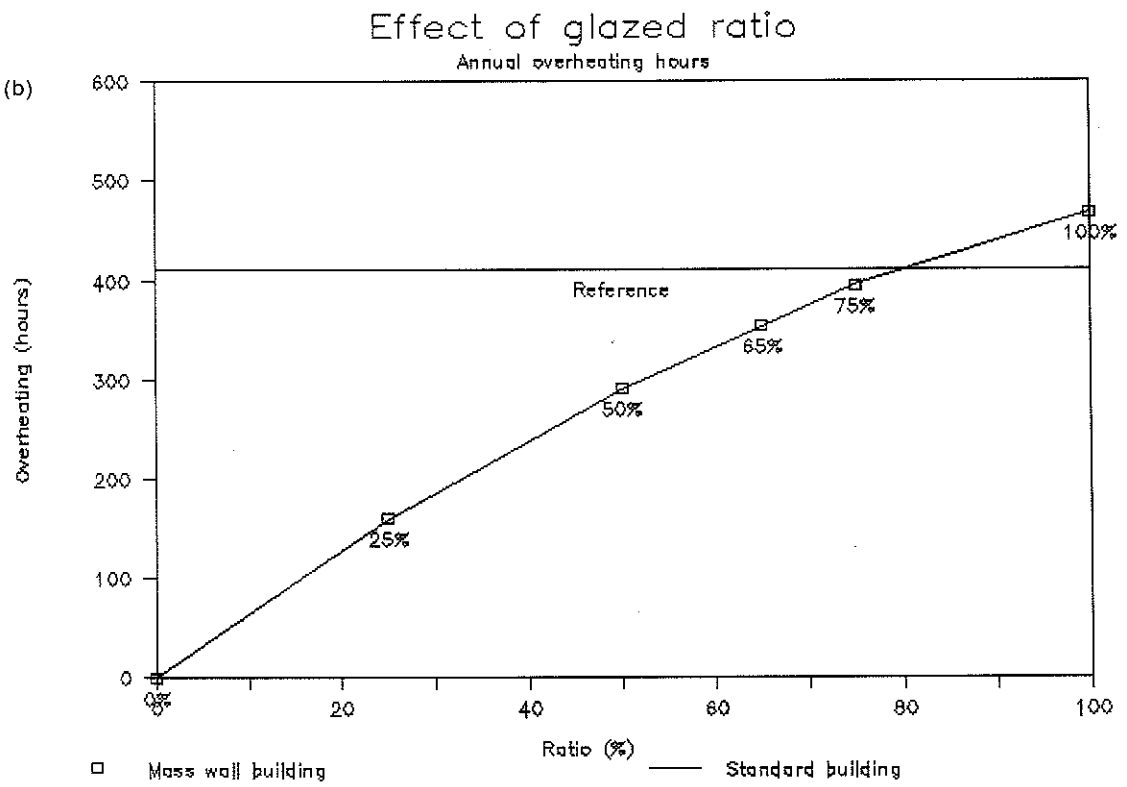


Fig. 17. Examples of sensitivity curves. (a) Annual heating load. (b) Annual overheating hours.

The evaluation criteria that allowed the objective comparison between several designs were choosen as

- the total heating load for the evaluation of the energy savings and
- the number of overheating hours in the offices (the most frequently occupied zone of the building) for the evaluation of thermal comfort.

For each parameter investigated, different values (generally five) were tested and the simulations results provided the "sensitivity curves" of the building. Examples of such sensitivity curves are given in Fig. 17 for both the energy and comfort evaluation criteria.

As a result of the optimization process, the design yielding the best energy performance of the building is characterized by:

- a south orientation,
- a double low-e glazing,
- a narrow buffer space (wall and glazing close to each other),
- a black wall,
- a 25% glazed ratio in the south facade, and
- an optimized control strategy of the heating system.

Furthermore, the building performance appears to be poorly sensitive with respect to the other parameters of the building.

Figure 18 shows the monthly heating load for three designs: (a) the "base" design (the building as it is), (b) the "reference" design (an equivalent building realized according to the Belgian construction standards), and (c) the optimized design. The results show that a 15% energy savings can be achieved when optimizing the design of this building. Furthermore, the calculation of the solar fraction has been performed by means of a simulation method. Therefore, the building is simulated twice. First, it is simulated with actual and complete weather data. Then, it is simulated again with an artificial data set in which the insulation values (global, direct, and diffuse) are set to zero. This second simulation yields the performance of the building if there was no sun. The comparison of the heating load in both cases yields the solar contribution to the heating load. The same procedure was applied for both the base case and the optimized case and the following solar fractions were obtained:

| Case | Solar fraction |
|---|---|
| Base | 0.29 |
| Optimized | 0.33 |

The same method can be applied to the internal gains, and the overall computation yields the yearly or monthly distribution of heat flows (solar, auxiliary, internal) for the different designs (Fig. 19).

## 8. CONCLUSIONS

### 8.1 *Measurements*

Measurements on the FUL building show that the building doesn't work as it should. The passive solar contribution to the heating load is reduced by several design mistakes. The mass wall doesn't collect enough

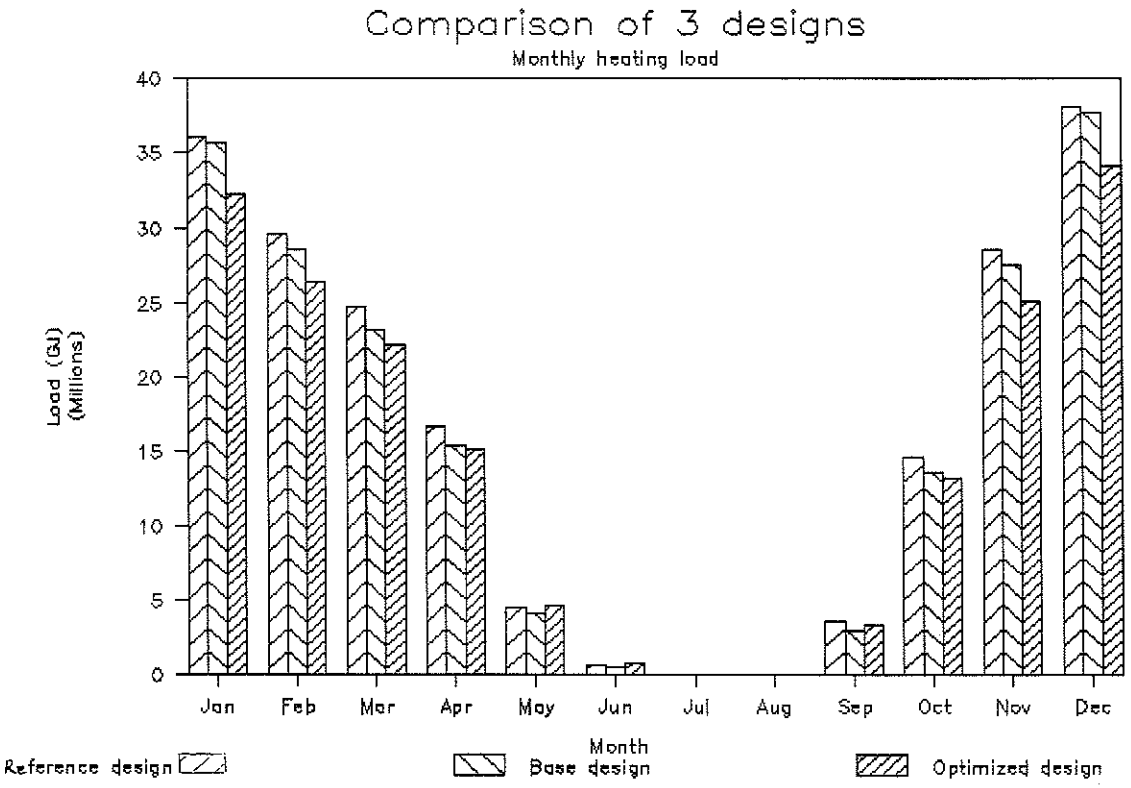


Fig. 18. Monthly heating load for three designs.

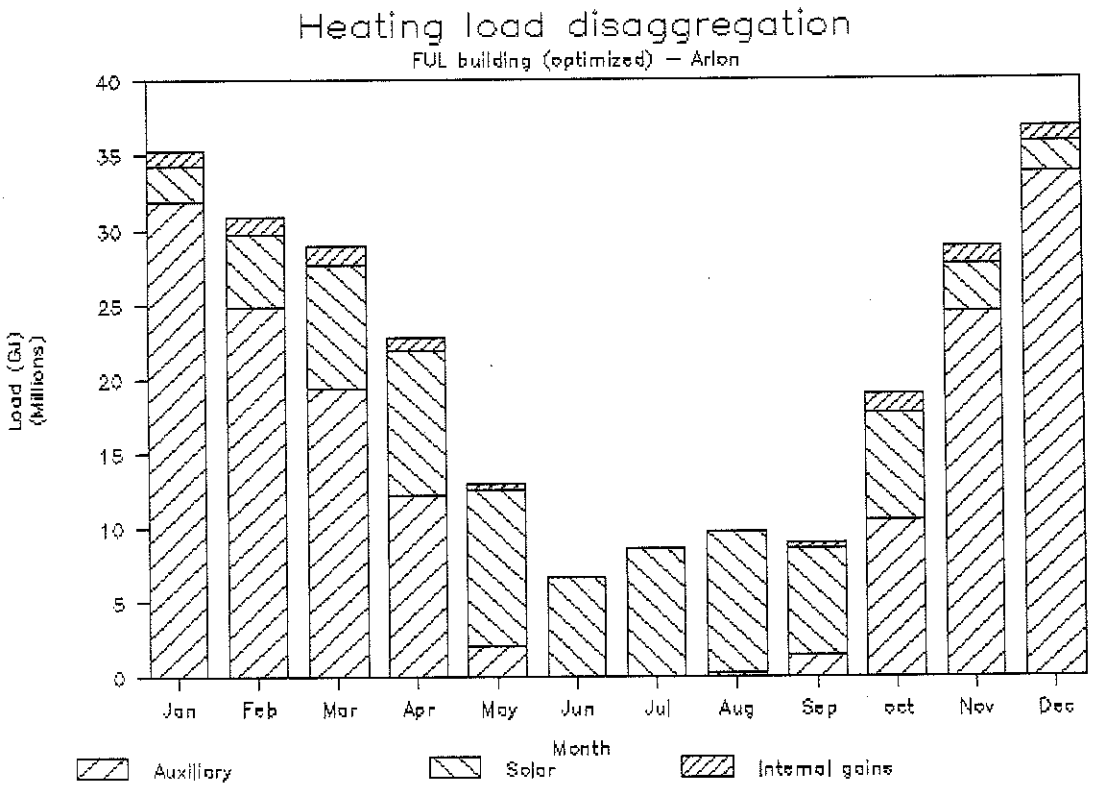


Fig. 19. (a) Monthly distribution of the heating load for the optimized design.

energy and the glazing quality is too poor to keep the solar gains inside the sunspace. Consequently, much of the solar gains entering the sunspaces are lost either by the wall itself (reflection toward outside), by the glazing, or by the ventilation ducts (heated by the sun and cooled by the air pushed outside). The behavior of the wall is nevertheless satisfactory in summer when it works as a damping device for the temperatures inside the auditoriums.

The auxiliary heating system doesn't work satisfactorily during the setback period. The problem has been located (bad functioning of a three-way valve) but has not been solved yet. More generally, an optimization of the different control systems (heating, venting, shading) should be performed in order to improve the passive solar behavior of the building.

Overheating is a major problem in this building as well, especially at the upper floor where the direct gain contribution is much more important than at the ground floor. Temperatures rising up to 35° Celsius have been recorded and most of the cooling devices (shutters, windows, ventilation) are shown not to be appreciated by the occupants. The comfort conditions are substantially better at the ground floor, especially in the auditorium during summertime. In these rooms, the temperature is kept close to a constant value despite the external temperature variations.

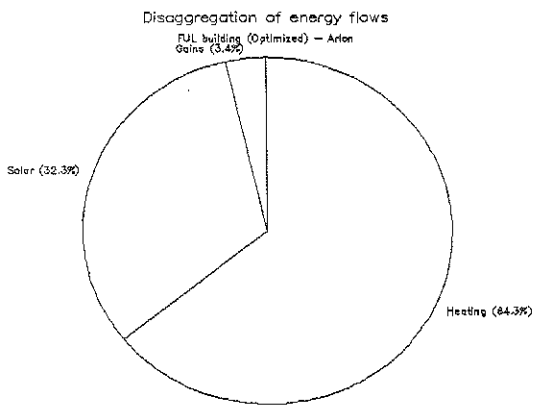


Fig. 19. (*Contd.*). (b) Yearly distribution of the heating load for the optimized design.

### 8.2 *Simulations*

Simulations of the FUL building have shown the theoretical solar fraction to be 29%. This is an appreciable result. A survey of the different parameters influencing the performance of the building and a systematic parametric analysis yield an optimization of the design. This optimized design results in a 15% energy savings compared to the base case. Once optimized, the building performs well, with a theoretical annual heating load close to 240 MJ/m$^2$ gross. Considering 70% heating system efficiency, this results in an estimated load of 340 MJ/m$^2$ gross, a good performance for a passive solar building in the Belgian climate. However, building energy optimization yields

worse comfort conditions, especially in the offices where the overheating frequency is substantially increased. Comfort in the auditoriums is not affected by building optimization.

### 8.3 *Synthesis*

This analysis has shown that a good combination of experimental results and computer simulation could work as a method for defining the optimum design of a mass wall building in the Belgian climate. Simulations allow extrapolations to be made of what has been measured while measurements establish a link with the real world. As a conclusion, it seems possible to design a mass wall building in the Belgian climate that would exhibit an annual heating load of less than 350 MJ/m$^2$ gross floor area.

*Acknowledgments*—This research has been funded by the Belgian Ministry of Economic Affairs (from 1987 to 1990) and by the Ministry of the Walloon Region (from 1990 to 1991). The authors are indebted to both organizations for their financial support.

## NOMENCLATURE

$A_{ve}$ area of the external glazing node
$A_{vi}$ area of the internal glazing node
$A_{w_0}$ area of the mass wall surface node
$A_{w_i}$ area of the mass wall internal nodes
$e_v$ thickness of the glazing
$e_{w_i}$ thickness of the mass wall nodes
$F_g(t)$ conversion factor between global horizontal solar radiation and global vertical solar radiation
$F'_{ve,\mathrm{sky}}$ view factor between the glazing and the sky
$F'_{vi,w_0}$ view factor between the glazing and the mass wall
$F'_{w_0,vi}$ view factor between the mass wall and the glazing
$F'_{w_{n+1},\mathrm{walls}}$ view factor between the mass wall and the other walls of the room
$h_{ve}$ convection coefficient at the external glazing surface
$h_{vi}$ convection coefficient at the internal glazing surface
$h_{w_0}$ convection coefficient at the mass wall external surface
$h_{w_{n+1}}$ convection coefficient at the mass wall internal surface
$S_H$ global horizontal solar radiation
$T_{ext}$ ambient temperature
$T_{ve}$ external glazing temperature
$T_{vi}$ internal glazing temperature
$T_a$ buffer space temperature
$T_{w_0}$ mass wall surface temperature, buffer space side
$T_{w_i}$ mass wall internal temperature
$T_{w_{n+1}}$ mass wall surface temperature, room side
$V_a$ volume associated with the buffer space node
$V_{w_i}$ volume associated with the mass wall nodes
$(UA)_{\mathrm{ground}}$ heat exchange coefficient with the ground
$(UA)_{\mathrm{roof}}$ heat exchange coefficient through the roof
$\alpha_{ve}$ external glazing solar absorptance
$\alpha_{vi}$ internal glazing solar absorptance
$\alpha_{w_0}$ mass wall solar absorptance
$\varepsilon_{\mathrm{sky}}$ sky emissivity
$\varepsilon_{ve}$ external glazing emissivity
$\varepsilon_{vi}$ internal glazing emissivity
$\varepsilon_{w_0}$ mass wall emissivity, buffer space side
$\varepsilon_{w_{n+1}}$ mass wall emissivity, room side
$\varepsilon_{\mathrm{walls}}$ room walls emissivity
$\lambda_v$ glazing thermal conductivity
$\lambda_{w_i}$ mass wall thermal conductivity
$(\rho C_p)_a$ air node thermal capacitance
$(\rho C_p)_{w_i}$ wall nodes thermal capacitance
$\sigma$ Stephan-Boltzmann constant
$\tau_{ve}$ glazing solar transmittance

## REFERENCES

1. J. Nicolas and J. P. Poncelet, Solar assisted heat pumps system and in-ground energy storage in a school building, *Solar Energy*, **40**, 117–125 (1988).
2. International Energy Agency Task XI, *Basic case studies*, Energy Technological Support Unit, Harwell Laboratory, Great-Britain (1989).
3. I. Bryn, An energy information system for atrium design, *Sun at work in Europe* **5**(4), 16–18 (1990).
4. International Energy Agency Task XI, Advanced case studies, *Proceedings of the Advanced Case Studies Seminar*, Databuild Ltd. (1991).
5. Ph. Andre, *"IDSOFT", un logiciel d'estimation des paramètres des systèmes dynamiques par des méthodes d'identification des processus*, Fondation Universitaire Luxembourgeoise, Arlon, Belgium (1989).
6. International Energy Agency Task XI, *Source book of examples and design insights*, International Energy Agency, Solar Heating and Cooling Program (1993).
7. Ph. Andre, J. Nicolas, J. F. Rivez, Application of identification methods for the determination of heat exchange coefficients in a passive solar commercial building, *Proceedings ISES* 1989 *Congress* (1990).
8. M. J. Delahunt, *Suncode-PC, a program user's manual*, Ecotope Inc. (1985).
9. P. Nusgens and L. Cotton, *MBDSA—Guide de l'utilisateur*, Université de Liège (1989).